Synchrotron Based X-Ray Strain Mapping in Fatigued Materials Subjected to Overloading

Thomas Tsakalakos, PI, Mat. Sc. & Eng. Dept, Rutgers University, Piscataway, NJ; 08854
Mark C. Croft Co-PI, Department of Physics, Rutgers University, Piscataway, NJ 08854;
Collaborators
Z. Zhong, National Synchrotron Light Source, Bldg. 725D, Brookhaven National Laboratory. Upton, NY 11973
R. Holtz, K. Sadananda NRL, Washington, DC

OVERVIEW

The application of high-resolution strain mapping in large engineering samples with both high-spatial and strain resolution is reviewed in this report using high-energy photons between 100 and 300 KeV on beam line X17B1 of Brookhaven National Laboratory. This was achieved by using Energy Dispersive X-ray Diffraction (EDXRD) methods and synchrotron radiation for the nondestructive measurement of residual stresses in engineering components. Examples of residual stresses profiles will be presented which include: laser and shot peening and fatigue crack stress fields. The presented results have been validated with other methods such as FE and other model predictions. This technique represents a significant development in the in life prediction of engineering structures including large naval structures.
KEY WORDS: Residual Stress, EDXRD, synchrotron, fatigue, weldments, laser peening, shot peening.

INTRODUCTION

One of the most significant components of the naval structure is the integrity of the weldments. Moreover the ability of the structure to endure the variable fatigue

loading of the ocean waves or landing overstresses during the life of the structure is as critical. In shipbuilding, aircrafts and ocean and land engineering, all welded structures suffer cracking by various types of in-service loadings, such as impact, fatigue and corrosion. Recently, observed cracking has been ascribed to fatigue cracking initiating at weldments. These fatigue cracks are either surface cracks or through-thickness cracks. It is for this reason that the prediction of fatigue performance of welded tubular joints used in the construction of naval structures has received such attention during the last few years. Structural design and experimental material mechanics are sufficiently advanced sciences so that catastrophic mechanical failure of structural elements is rare. However, under cyclic or variable loading, well below static load tolerance levels, the almost inevitable failure of structural materials due to fatigue cracking is still not understood well enough to accurately predict the key question of when failure will occur. Attaining a reliable prediction methodology for fatigue crack growth will have tremendous benefit for the safety and life cycle costs of complex systems such as naval structures.

At the very heart of the of the fatigue crack growth prediction problem is the singular behavior of the in the stress/strain field in the vicinity of a crack tip and the plasticity thereby produced (Suresh, 1998). It is noteworthy that many years of prodigious modeling efforts in this field have been carried forth virtually without any experimental probe that could directly measure, with sufficient resolution, in the interior of a specimen, the crack tip strain fields upon which the models are based. Quantification and model based descriptions of fatigue crack growth have most certainly had some success but it has been through the resourceful exploitation of strain/stress measurements remote from the crack tip, along with other indirect and macroscopic measurements (Suresh, 1998). The main purpose of this report therefore, is to present a comprehensive review of the high resolution EDXRD techniques on a variety of

applications including fatigue crack strain fields in the interiors of steel specimens, in laser/ shotpeened materials that clearly demonstrate that strain field mapping at the relevant length scale is now possible and in sufficient detail to be useful for theoretical analysis.

On the other hand, catastrophic failure of cyclic load-bearing components is, more often than not, near surface initiated. In particular, tensile surface strains/stresses, arising in the manufacture, processing or duty cycle of the component, greatly accelerate the surface-initiation and growth of cracks (Deslaef, 2000). Since antiquity it has been empirically recognized that surface hardness/durability could be enhanced by impact-cold-working. The systematic improvement of fatigue life by shot and laser peening has been very well understood by the near surface compression. The characterization of the surface compression /toughening as a function of the peening intensity has been studied exhaustively over the years to optimize performance of a multitude of components varying from dental picks to airplane wings. Characterization of the detailed magnitude and depth of the shot peening surface compression are crucial to the systematic improvement of this already highly successful surface toughening process (Tsakalakos, 2002). Such characterization rests on the same repertoire of techniques used in the more general field of residual strain/stress (RS/S) depth profiling (Croft, 2002; Prime, 1999; Whithers, 2001). Many of the most frequently used techniques in this area are explicitly destructive, and involve theoretical modeling of the strain fields accompanying material removal (e.g. hole drilling and layer removal) (Croft, 2002). Conventional X-ray and neutron scattering have traditionally been the only direct (i.e. involving actual lattice parameter measurements), non-destructive methods for strain profiling as a function of depth into a material (Croft, 2002; Prime, 1999; Whithers, 2001). Unfortunately, the short penetration depth of the former (< 0.01 mm), and the large sampling volume (~1 mm^3) of the latter make their applicability to shot and laser peening studies quite demanding. The focus of this report is on the application of Energy Dispersive X-ray Diffraction (EDXRD) in residual stress measurements in various deformation processes such as fatigue shot or laser peening.

BACKGROUND

In the last few decades, volumes of theoretical and empirical work have been done on residual strain profiling. Fig. 1 is a summary of overviews (Kandil, 2004; Leggatt, 1996; Prime, 1999), and illustrates the scope of the residual strain-profiling problem.

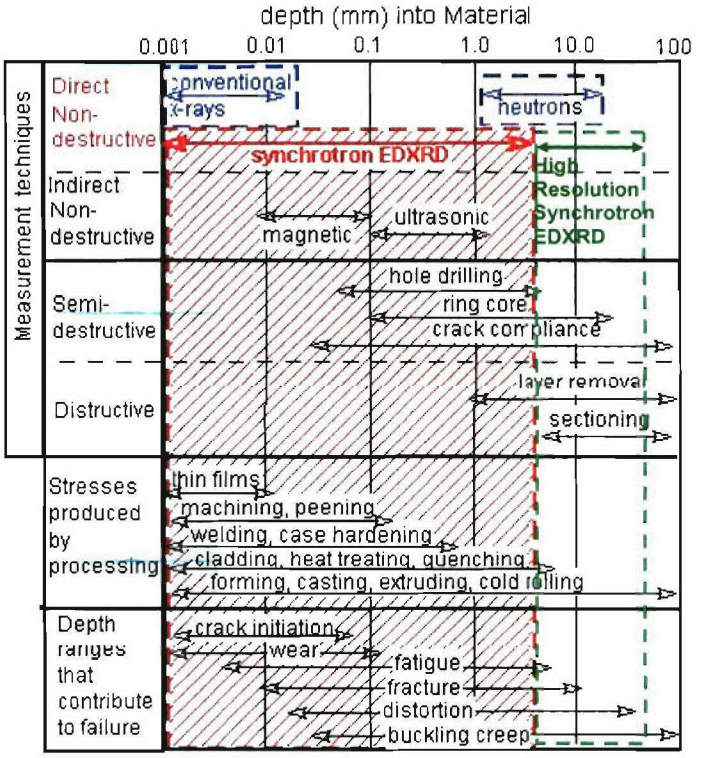

Fig.1 A schematic, summarizing residual strain (RS) sources, relevance, and means-of-measurement as a function of depth below the surface of a material. Specifically the summary is divided into: the RS measurement techniques, shown at the top; the materials processing origins of the RS's at the center; and the classes of material-component failure that can result from RS's at the bottom. The direct-nondestructive conventional x-ray and neutron scattering methods are highlighted. The red-shaded region emphasizes the crucial range/relevance of the direct-nondestructive EDXRD techniques discusses in this report. The green-shaded area represents the range of applicability of the **new high resolution EDXRD technique developed under our ONR funding.**

This figure summarizes concisely the depths (into a component) relevant: to measurements techniques for residual stress analysis; to various manufacturing and processing methods; and finally to typical component failure mechanisms. Only a few simple points from this Fig. 1 will be emphasized here. Many of the most powerful techniques are destructive and involve theoretical modeling of the strain fields accompanying material removal/modification (e.g. Hole drilling and layer removal). Conventional x-ray and neutron scattering have traditionally been the only direct (i.e. involving actual lattice parameter measurements), non-destructive methods for strain profiling as a function of

depth into a material. The short penetration depth of conventional x-ray analysis limits its use to the very near surface region (see Fig. 1). The weaker scattering of the neutrons allows deep penetration (to tens of mm), however it also precludes sampling volumes of less than about 1 mm^3, thereby limiting both spatial resolution and lower limit of applicability. Thus, here-to-fore there was a gaping hole in spatial scales and resolution in the direct/non-destructive methods available for strain-field depth profiling.

In recent years high intensity/energy synchrotron radiation and high resolution synchrotron EDXRD has begun to be used for deeply penetrating X-ray diffraction strain profiling (Kuntz, 1996; Pyzalla 2000; Whithers, 2001; Zakharchenko, 2002). The high count rates, from small diffraction volumes, and simultaneous multi-line diffraction spectra achievable using EDXRD has made it one of the prime techniques for such strain field depth profiling. The high resolution synchrotron radiation x-ray diffraction techniques have emerged which provide a direct, nondestructive, probe of local strain tensor (Tsakalakos 2002).

Table 1 Comparison of Residual Stress Measurement Techniques

Residual Stress Measurement	Destructive	Contact	Portable/Lab Equipment	Speed	Reliability	Cost
Layer Removal / Sectioning	Yes	Yes	Lab Low	Med.	Poor/ Med.	Low
Hole Drilling	Yes	Yes	Both Low	Fast	Poor/ Med.	Low
Synchrotron	No	No	Lab/Spec Medium	Fast	High	Med.
Neutron Diffraction	No	No	Lab/Spec High	Slow	High/ Med.	High
X-ray Diffraction	No	No	Both Low	Fast	Poor/ Med.	Med.
Ultrasonic	No	No	Both Low	Fast	Poor	Low
Raman	No	No	Both Med	Fast	Poor	Med.
Magnetic	No	No	Both Medium	Fast	Poor	Med.

The applicability of the high resolution EDXRD techniques is shown in Fig. 1 as green-shaded area. The penetration is as large as a few centimeters in steels and several tenths of centimeters of aluminum alloys. Moreover, the new high x-ray intensity synchrotron techniques allow for much smaller probing volumes, enabling a higher resolution mapping of the locally singular behavior near the crack tip (Croft, 2005). The benefits of the high-resolution EDXRD can be also seen in Table 1 where a comparison of benefits, advantages and limitations are presented for most key residual stress measurements techniques.

These techniques have been applied to a number of problems including selected proof of principal applications to strain field mapping in the vicinity of fatigue cracks (Croft, 2005; James, 2004; Steuwer, 2004). While some previous conventional x-ray diffraction studies have provided useful insights into the near-surface strain field variations in the vicinity of fatigue cracks (Allison, 1979; Ramos, 2003; Wang, 1999), the deeply penetrating, high energy synchrotron experiments have demonstrated the ability to probe the fatigue crack strain fields well within the interior of specimens. This will be quite important to the future of fatigue damage research because the vanishing of the near surface-normal stress component ("plane-stress condition") makes the crack tip behavior near a surface fundamentally different from the interior crack tip behavior where a "plane-strain" condition holds (Bao, 1998; Makabe, 2004).

This report discusses the detailed components of the EXRD experimental technique variation of the fatigue crack strain fields in the interior of a series of 4140 alloy steel specimens. In particular these specimens were prepared to study the "overload effect" in which a single tensile overload cycle is known to retard, for a time, subsequent crack growth (Sadananda, 1999; Lang, 1999). Understanding the role of such load amplitude variations in shaping the stress fields is key to important practical fatigue crack growth prediction (Skorupa, 1998, 1999). The synchrotron based x-ray diffraction results presented here provide a picture of the fatigue crack strain field variations at a heretofore unprecedented level of detail.

EDXRD RESIDUAL STRESS MEASUREMENTS

It has been widely reported (Croft, 2005) that synchrotron-based RS measurement techniques have made significant progress for improving the quality and reliability of residual stress measurements. **The ability to measure and monitor the development of residual stresses in a component at various stages of manufacture is a key issue.**

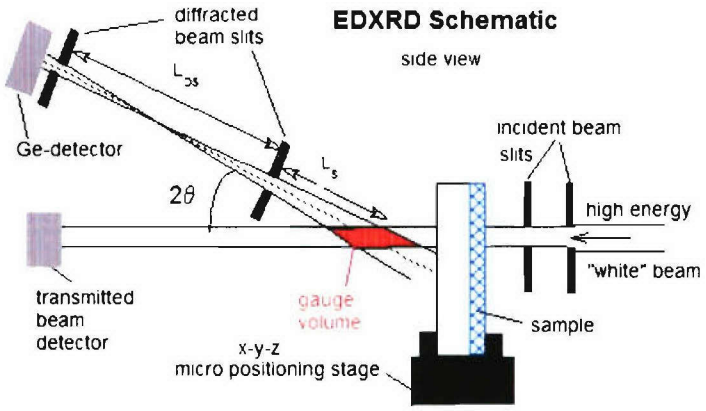

Fig.1 A schematic of the EDXRD experimental apparatus (X17B1 at NSLS) used in these experiments. The high-energy, "white" x-ray beam enters at right. The micro- swept through this scattering volume while the EDXRD spectra are collected by the energy-dispersive-Ge detector.

Synchrotron based energy dispersive X-ray diffraction (EDXRD) has emerged as a promising new method for residual stress analysis due to its high intensity, its high parallelism, and its simultaneous collection of many Bragg lines (Kuntz, 1993; Pyzalla, 2000; Tsakalakos, 2002). Our group has been applying the EDXRD technique to the profiling of fatigue crack strain fields, Laser and shot peened materials, large naval and other engineering structures, at the Brookhaven National Synchrotron Light Source (NSLS) at beam line X17-B1. A schematic for of the X17-B1 experimental apparatus is shown in Fig. 1. Several parts of the apparatus should be noted. The wiggler high energy white beam enters from the right. (Here, it should be noted that the superconducting wiggler insertion device at X17 produces high intensity X-rays in the 30–300 KeV energy range which is essential to these EDXRD measurements. The incident and diffracted beams are tightly collimated by two slits each, thereby defining the small-size of the gauge volume.

The beam intensity transmitted through the sample is monitored by a detector so that a radiographic profile (referred to as a transmission profile, TP) of the sample can be constructed for precise positioning with respect to local structures, like a fatigue crack in the present study. The curial crack-locus and -tip position, in the studies reported here, were mapped out using a set of transmission profiles.

In EDXRD, the incident beam and detector remain fixed at the desired fixed scattering angle 2θ. For typical small thickness samples $2\theta=12^{0}$. However, **for large engineering bulk structures of up to 2 inches in steel and up to 2 feet in aluminum alloys a $2\theta=6^{0}$ special set up was used for deep penetrations**. Polychromatic radiation is incident on the sample and the high resolution solid state Ge detector analyzes the energy of the resulting diffraction. The dramatic increase of high energy photon of representative diffraction spectrum for a steel sample is shown in Fig.2. A fatigued-over-loaded 4140 steel sample is illustrated in Fig. 3 ($2\theta=12^{0}$), where the Miller indices of the individual Bragg reflections are indicated. The stability of the stationary incident and diffracted beams facilitates the high precision of the analysis of the material lattice parameter, a ($\Delta a \sim 0.0001$ A).

The cross section dimensions of the diffraction gauge volume can vary from 5 μm to a few mm depending on the application.

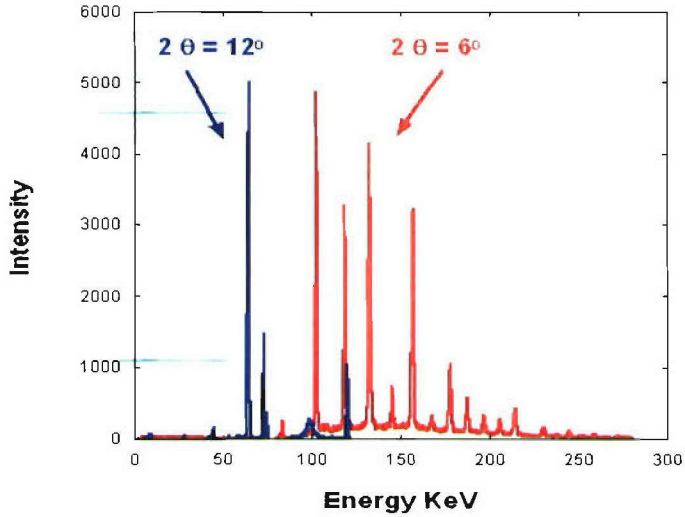

Fig. 2 Steel EDXRD spectra showing the dramatic shift to high energy photons for the high resolution EDXRD technique ($2\theta=6^{0}$).

Bragg's Law (below) relates spacing between planes in a crystal lattice d_{hkl} to the energy of the diffracted photon E and the fixed scattering angle θ. The relation between the Miller indexed inter-atomic-plane spacing (d_{hkl}) and the corresponding Bragg reflection energy E_{hkl} is given by

$$E_{hkl} = \frac{hc}{\lambda} = \frac{hc}{2\sin\theta} \cdot \frac{1}{d_{hkl}} \qquad (1)$$

where $\{hkl\}$ are the miller indices identifying the crystalline planes, E_{hkl} the energy of an $\{hkl\}$ reflection, h is Plank's constant, λ is the wavelength, d_{hkl} is the $\{hkl\}$ lattice spacing, c is the speed of light, and 2θ is the scattering angle which is very small in the 3.6°- 15°range ($2\theta=12°$ or 6^{0} in our case depending on the application).

For E_{hkl} given in KeV and d in Angstroms, the above equation becomes:

$$E_{hkl} = \frac{6.199}{\sin\theta} \cdot \frac{1}{d_{hkl}} = const. \cdot \frac{1}{d_{hkl}} \qquad (2)$$

Each crystal phase possesses a unique set of *d* spacings enabling differentiation. When a known experimentally scattering angle 2 θ is fixed, 6.199/sinθ becomes a constant. That means a particular crystallographic plane with a lattice spacing d_{hkl} diffracts at a particular correspondent energy E_{hkl}. Thus, measuring the center of gravity of peak energy at the fixed angle allows the calculation of lattice spacing. Strain can be determined from the shifts in peak energy:

$$\epsilon_{hkl} = -\left(\frac{\Delta d}{d_0}\right)_{hkl} = \left(\frac{\Delta E}{E}\right)_{hkl} \qquad (3)$$

where $\Delta d = d - d_0$ is the change in the lattice spacing, d_0 is the lattice spacing of the stress-free materials, $\Delta E = E_0 - E$ is the correspondent peak shift and E_0 is the center of gravity of peak of stress-free materials. Strain tensor ϵ_{ij} can be determined by measuring strain in different directions of the samples. Then the stress tensor σ_{ij} can be calculated by Hooke's law $\sigma_{ij}=C_{ijkl}\,\varepsilon_{kl}$.
Evaluation of d_0 is achieved by EDXRD measurements of specially prepared stress free materials, or trough using equilibrium equations etc. Details of methods for d_0 estimation are shown in references (Croft, 2002; Prime, 1999; Whithers, 2001).

RESIDUAL STRAIN/STRESS DISTRIBUTIONS OF OVERLOAD/FATIGUE PLASTIC ZONE IN CT 4140 STEELS.

One of the major reasons for the inability to predict the fatigue crack growth (FCG) behavior of many industrial and naval components and structures and thus the inability to develop of safety cases and the successful use of engineering critical assessments is due to the lack of understanding the influence of a tensile overload on fatigue crack growth. Most of the experimental observations of the effect of a single tensile overload applied during constant-amplitude high-cycle fatigue on the subsequent crack growth rate show a retardation of FCG (Sadananda, 1998; Vasudevan 1994).

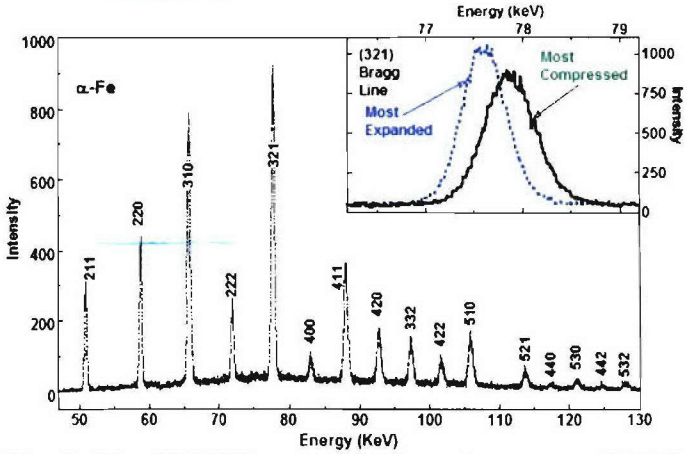

Fig. 3. The EDXRD spectrum from the center of 4140 steel specimen which has been fatigued and subjected to a single 200% overload cycle. The Miller indices of cubic a-Fe are shown. Inset: expanded views of the 321 Bragg lines, at two positions in the fatigue crack plane, are shown: at a point in front of the crack tip where the maximum tensile strain is observed; and at the center of the overload plastic zone where the maximum compressive strain is observed. Note the lattice dilatation shifts (the shift to higher energy corresponds to a smaller lattice parameter). Note the intensity scale is absolute and the broadening and decreased maximum-intensity of the peak in the plastic zone is intrinsic and will be discussed below.

Table 2 Materials constants and fatigue test parameters.

4140 steel :
E ≈ 207 GPa, ν= 0.3; σyield~ 650 MPa;
KIc ≈ 65 MPa m1/2; tensile strength 1020 MPa,
CT:high K
Kmax= 39.6 MPa $m^{1/2}$, Kmin=3.96 MPa $m^{1/2}$, ΔKappl=36.6 MPa $m^{1/2}$, R=0.1
KOL=2Kmax= 79.2 MPa $m^{1/2}$
$r_{poverload}$=2.4 mm, $r_{pmonotonic}$=0.6mm

The Materials constants and Fatigue Test Parameters are shown in Table 1.

r_p=monotonic plastic zone size= $(1/2\pi)(K_{max}/\sigma_y)^2$ (4)

For 100% overload

$r_{p\text{-}overload}$=plastic zone size= $(1/2\pi)(2K_{max}/\sigma_y)^2$ (5)

As shown in Table 2 for the High-K CT specimen the calculated monotonic plastic zone size is r_p=0.6 mm and the overload plastic zone size r_p=2.4 mm.
An initial acceleration of the crack is frequently reported, followed by a deceleration to a minimum level and a gradual acceleration to the pre-overload crack growth rate. The precise micromechanics of this phenomenon are not fully understood and in particular the influence of

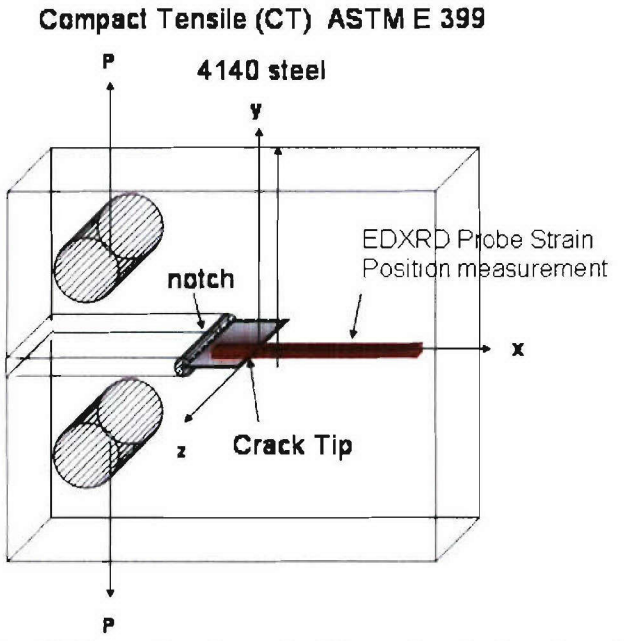

Fig. 4 CT sample schematic, illustrating the location of the crack near the notch, and the position where the EDXRD measurement was performed.

specimen thickness on retardation behavior is the subject of some controversy.

An understanding of this behavior is required in order that adequate account can be taken of the variable-amplitude response of many components and structures in engineering-critical assessments and residual life estimations.

The CT sample geometry and probe position of EDXRD strain distribution measurements are shown in Fig. 4.

The EDXRD stress mapping of plastic zone along the x-axis of a Compact Tensile (CT) specimen of 4140 steel after 100 % overload and measured at zero load (see insert) is shown in Fig. 5.

The aim of this work was to measure residual stress and strains in the vicinity of plastic zones accurately which in turn will allow for development of theoretical understanding of this phenomenon and thus develop the framework for fatigue life prediction in variable amplitude response of engineering components (Noroozi, 2005; Stoychev, 2005).

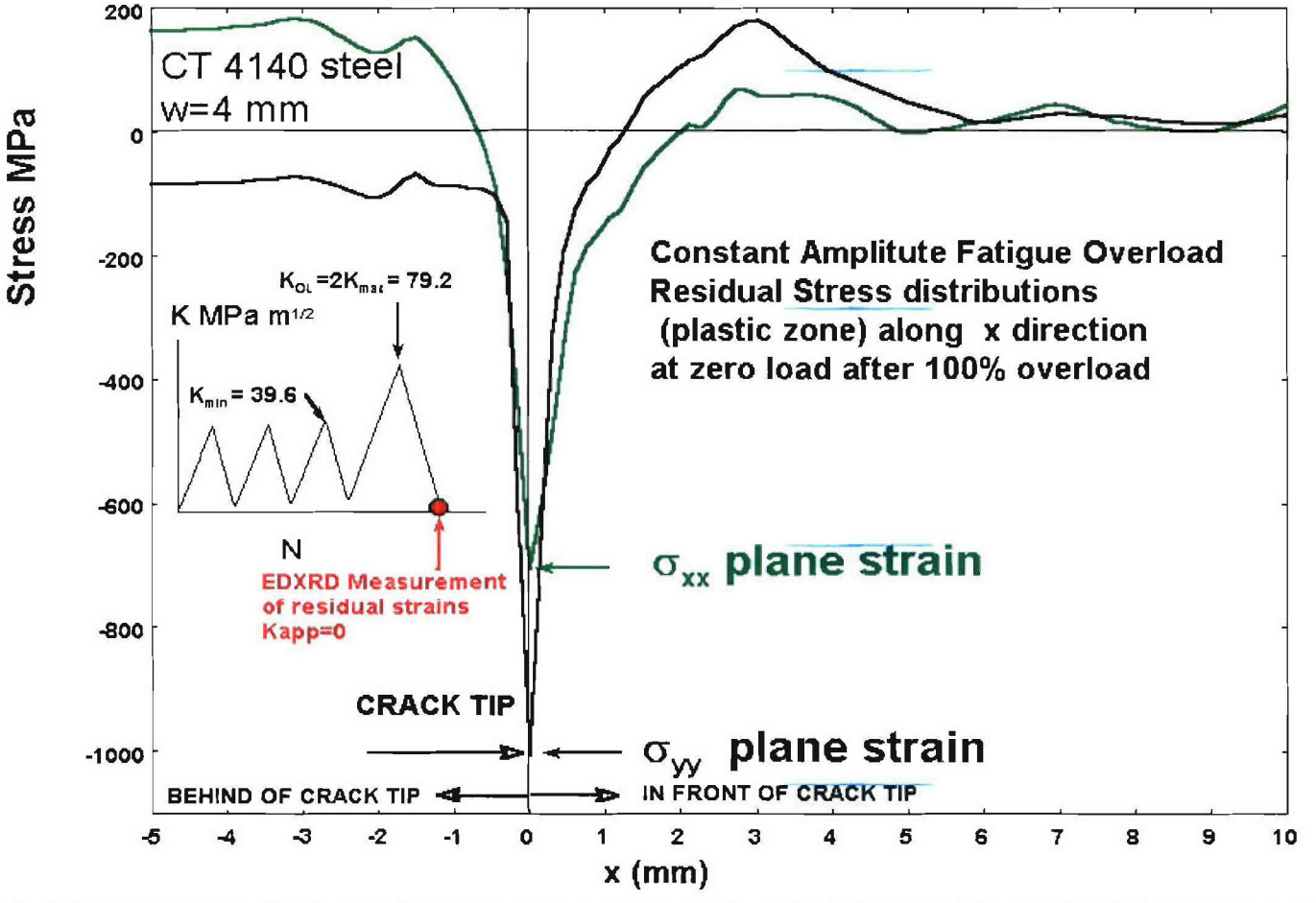

Fig.5 CT residual stress distribution for plane strain near crack of overload CT steel. The details of the Fatigue overload experiment and measurement location is shown in the insert.

STRAIN MAPPING IN 4140 STEEL EDXRD RESULTS DEPICTED IN FIGURES 5, 6 & 7

1. In front of the crack stress distribution σ_{xx} outside the plastic zone shows elastic tensile behavior as expected from the linear fracture mechanics theory despite the fact that the corresponding σ_{xx} goes asymptotically to zero stress from compressive behavior.
2. The experimental value of the overload plastic zone size is $r_{pexperimental}$=3 mm as shown in Fig. 5 form the which is consistent with the theoretical value of $r_{poverload/theoretical}$=2.4 mm. Actually the plastic zone is expected to be larger due to the relaxation of the stress over the plastic zone region. For elastic perfectly plastic behavior $r_{poverload}=2\ r_p$
3. The maximum compressive stresses near the crack tip for the Plane strain case: σ_{xx}=705MPa, σ_{yy}= 1007 MPa , σ_{zz}=514 MPa

These values suggest a high triaxiality effect for the plane strain case the plastic constrain factor p.c.f=1.56 which is close to Irwin's approximation of 1.68 where as the corresponding p.c.f for plane stress is 1.2.

4. The stresses behind the crack are approximately σ_{xx}=180 MPa, σ_{yy}=-70 MPa

The small value of compressive stress σ_{yy}=-70 MPa observed behind the crack tip might be due to the fact that first the probing volumes for the EDXRD strain measurements ε_{xx} ε_{yy} are different and second the precise location of the same point of measurement is very difficult. Near the crack surface the variation of the strain fields are very sharp. Indeed 150 μm away from the crack surface along the y direction the ε_{xx} and ε_{yy} and therefore σ_{xx} and σ_{yy} are exactly zero. This behavior is observed for fatigued, overload-fatigued and fatigued-overload-fatigued deformation. The residual stress distributions behind the crack tip are independent on the fatigue history, thus suggesting a that major driving force of fatigue crack growth is due to the residual stress distributions in front of the crack (contour plastic zone depicted in Fig. 5) (Noroozi, 2005; Stoychev, 20052005; Vasudevan, 1994).

A high spatial resolution contour plot of ε_{yy} (50 μm x 50 μm diffraction gauge cross section) is shown in Fig. 6. The feature characteristics in Fig. 6 are in accordance with the strain profile features predicted by FEM and other modeling as shown in Fig. 7. The at-crack (or wake) ε_{yy}-anomaly (labeled C/1) can be seen extending along the crack entering the figure from the left. The regions of positive ε_{yy} values, bordering the crack at a distance of ~0.5 mm from the crack, are labeled D/2. The now much sharper epicenter of compression at the

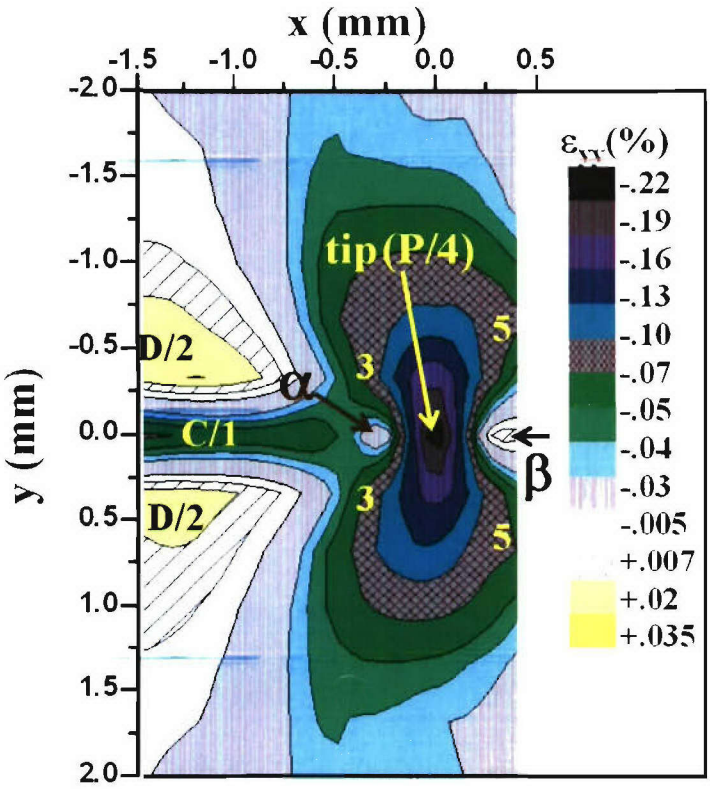

Fig. 6. A high spatial resolution contour plot of the ε_{yy} strain component near the crack tip of the Fatigue/Overload specimen.

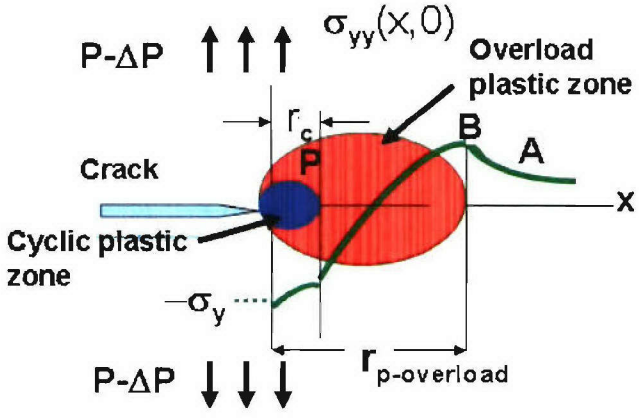

Fig. 7 A schematic of crack tip residual stresses after an overload cycle (similar to those found in Suresh (1994) and Verma (2002). The qualitative spatial locus of the crack tip (at the origin), and cyclic, and monotonic plastic zones are shown. Superimposed, without scale, is the qualitative x-variation of the y-component of the stress in the y=0, crack plane, $\sigma_{yy}(x,0)$. Note the stress variation in the elastic-far-field regime (A), at the monotonic plastic zone boundary (B), inside the monotonic plastic zone (B'), and inside the cyclic plastic zone (P).

tip is noted and the wide extension of the negative-ε_{yy} region extending vertically from the tip is clear.

The β-type tensile dip, extending toward the tip from the front, is much better articulated than the textbook schematic of fatigue crack growth modeling depicted in Fig. 7. The similarities of stress behavior in Figs.5,7 are remarkable. Finally the dramatic positive peak α-feature appears as a sharp island interposed between the C/1-structure along the crack and the large compression at the tip. The spatial extent and positioning of the α-type tensile dip suggest that it is related to the constant amplitude process zone which created the wake-effect but which has been modified by the imposition of the large compressive stress of the overload plastic zone.

The detailed strain mapping presented herein is for the ε_{yy} strain component variation, parallel to the principal crack driving stress, with selected ε_{xx} strain component measurements providing some insight into the complex multi-axial deformations that occur The thrust of this study is that the detailed mapping of the near-crack-tip behavior in the case where the residual strain field of a single-overload cycle plays a prominent role in modeling and life prediction of fatigue crack propagation zone (Noroozi, 2005; Stoychev, 20052005; Vasudevan, 1994).

RESIDUAL STRESS DISTRIBUTIONS IN SHOT AND LASER PEENED MATERIALS

Characterization of the detailed magnitude and depth of the shot and laser peening surface compression are crucial to the systematic improvement of this already highly successful surface toughening process in engineering and naval structures.

Shot and laser peening involves dynamic deformations between the hard spherical particles or high energy laser pulses metallic substrates, which results in layer 1 undergoing plastic flow while layer 2 is deformed elastically as shown in Fig. 8. The indentation at the

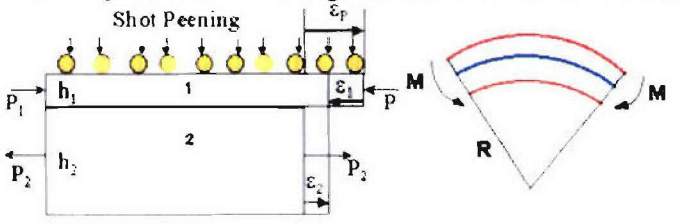

Fig.8 Schematic of model for shot peening strains/stresses and bending moment and radius of curvature for peened material.

impact area is the result of local plastic deformation that causes an in-plane expansion of the region, which is restrained by deeper adjacent regions that are not plastically deformed. The restraining of the in-plane expansion leads to a compressive straining of layer 1 which is extremely beneficial for failure prevention in engineering components.

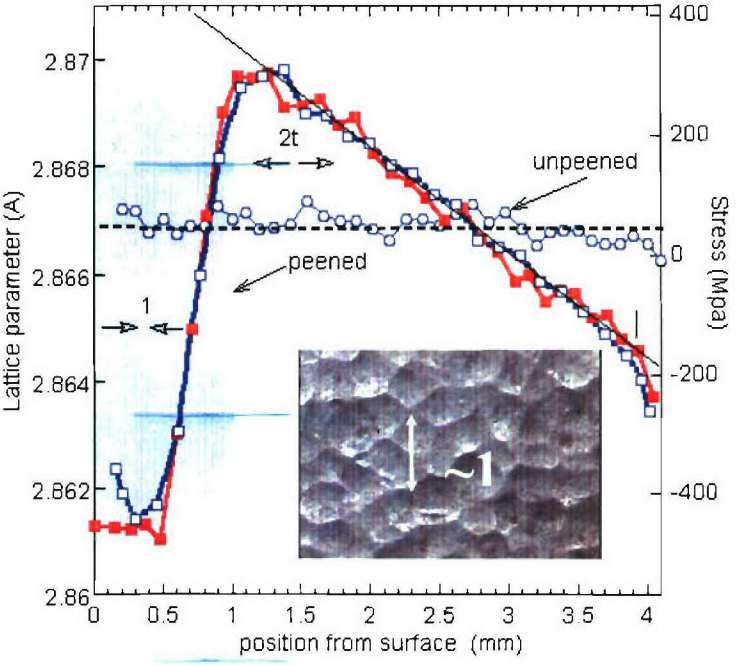

Fig. 9 Measured lattice parameter (2 separate scans – open and closed squares) and calculated stress profile for a 3.85mm thick spring steel placket peened with 1.4mm hard steel shot. The stress results for an unpeened placket are also shown that verifies the expected lack (zero) residual stresses in the unppened sample. A photomicrograph of the peened surface of the 3.85 mm thick specimen is inserted.

As expected from the simple model, the underlying steel (region 2) responds to the peened layer elastically, with the bending moment creating a linear elastic strain vs. position in region 2 given by $a = a_0 (1 - y/R)$.

Least squares fitting the linear portion of the region 2 data yields a microscopically-determined curvature of R=1530 mm, in quite good agreement with the macroscopic Almen Gauge curvature (R_A=1650 mm). This is an excellent quantitative validation of EDXRD method.

The larger-shot-size/deeper-plastic-layer correlation is dramatically apparent in Figure 10(a). Two compression depth indicators are labeled by arrows in the figure; the depth of first onset of the compressional deviation; and the compression half step depth.

Clearly the data supports a direct correlation between the plastic compression depth and the shot size.

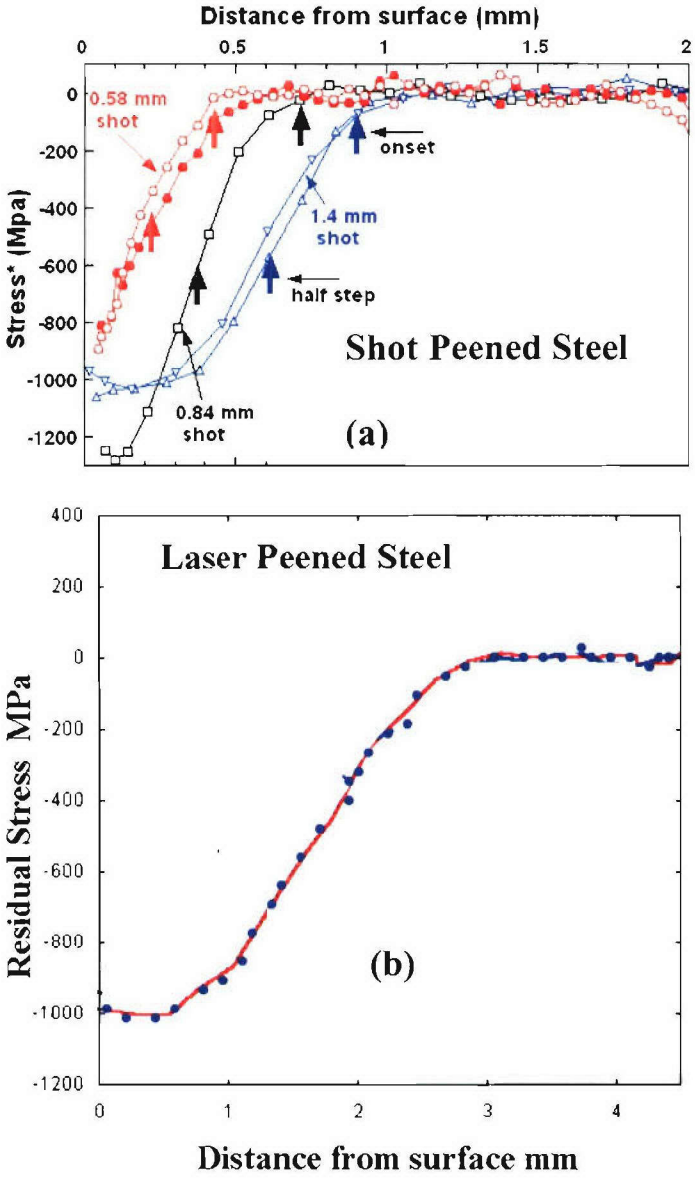

Fig. 10 (a) The stress profiles for the samples in the previous figure with the linear elastic components subtracted. Note that results for both surfaces of the double peened sample are included. The arrows mark the compression onset and half-step depths. (b) Residual stress measurement of laser peened spring steel. Note the dramatic enhancement of the compressive region of the laser peened steel.

The calculations of Al-Hassani, (1981) predicted an essentially linear relation between shot size and plastic zone depth. Such a linear correlation is supported by our limited study. Fig. 10(b) shows the dramatic increase of the compressive region from 0. 8 mm in shot peened materials to about 3 mm in the laser peened samples while maintaining large compressive stresses of the order of 1 GPa.

CONCLUSIONS

The results presented here provide a detailed picture of a **high resolution EDXRD experimental technique** on a variety of applications including fatigue crack strain fields in the interiors of alloy steel specimens, in laser and shot peened materials that clearly demonstrate that strain field mapping at the relevant length scale is now possible and in sufficient detail to be useful for theoretical analysis.

The detailed fatigue crack strain field, how it changes with an overload cycle and further evolves with subsequent fatiguing. These results, along with others in this ongoing study, yield actual microscopic strain field profiles to compare in detail with theoretical models. This unprecedented level of detail in the analysis of the internal strain fields that govern fatigue crack growth is important for materials science. The wealth of structure in these strain measurements will provide beneficial support for theoretical and modeling studies. Moreover, in view of the scarcity of facilities in the world capable of such strain field mapping, and in recognition that a large premium is placed upon high/high intensity synchrotron beam time, it is crucial to focus efforts on well articulated regions of interest such as those pointed-out in this work.

It is instructive to make a direct and simple correlation between crack growth and the overload strain field map in thick samples using a scattering profile method discussed previously (Tsakalakos, 20002). The beam intensity transmitted through the sample was monitored by a detector so that an in-situ radiographic profile (referred to as a transmission profile) of the sample could be constructed for precise positioning with respect to the fatigue crack and its tip. The precision mapping out of the crack-locus and crack-tip position was crucial to the detailed strain field mapping studies reported here, and will be discussed at length elsewhere.

In the ε_{yy} measurements reported here the x-y cross-section of the diffraction (gauge) volume was a 200 X 60 μm^2 rectangle. The z-y gauge volume cross-section was an elongated regular parallelogram (of 60 μm on side) with the maximal z extent being ~300 μm. The measured ε_{yy} values should therefore be considered as averages over these dimensions. The scattering vector, in this case, was inclined at only 6° with respect to the y-direction yielding, to an excellent approximation, the ε_{yy} strain component. The selected ε_{xx} strain component measurements presented here, to illustrate the importance of the strain/stress anisotropies in this problem, were

performed with the x-y collimation slits being as small as 50 X 50 μm^2 square.

Finally, recent experimental results of Residual Stress Distributions in similar and dissimilar welments have been obtained at X17B1 beam line of Brookhaven National Laboratory, (these results still under analysis). These results are on real engineering naval structures that further prove the applicability of the high resolution EDXRD technique in real life engineering components. The analysis involves structures which consist of parts with thickness over two inches in steels and over 12 inches in aluminum alloys. The in-situ residual stress measurements of such large scale are expected to have an enormous impact on our understanding of complex deformation modes in large engineering structures. The elucidation of the origin of combined stress and chemical effects represents a breakthrough in life prediction of every aspect of naval, industrial and societal materials needs.

ACKNOWLEDGEMENTS

We gratefully acknowledge the support of the Office of Naval Research (ONR) under Contract No. N00014-04-1-0194. The PI and Co-PI would also like to acknowledge detailed conversations with Dr. A. K. Vasudevan, I. Zakharchenko, A. Fast, N. Jisrawi, J. Skaritka, K. Sadananda, R. Holtz, G. Glinka and D. Kujawski and many other scientists and colleagues involved in this research endeavor.

REFERENCES

Al-Hassani, STS (1982). "Mechanical Aspects of Residual Stress Development in Shot Peening," *1st Int. Conf. On Shot Peening,* Paris, Pergamon Press Oxford, New York, pp 583 - 602

Allison, JE (1979). "Measurement of crack-tip stress distributions by X-ray diffraction," *Fracture mechanics, Proceedings of the Eleventh National Symposium,* Blacksburg, VA, pp. 550-562

Bao, H, and McEvily, AJ (1998). "On plane stress–plane strain interactions in fatigue crack growth, " *Int J. Fatigue,* Vol 20, pp 441-448

Croft, M, Zakharchenko, I, Zhong, Z, Gulak, Y, Hastings, J, Hu, J, Holtz, RL, DaSilva, M, and Tsakalakos, T (2002). "Strain Field and Scattered Intensity Profiling with Energy Dispersive X-Ray Scattering, " *J. App. Phys.,* Vol 92 , pp 578-586

Croft, M, Zhong, Z, Jisrawic, N, Zakharchenko, I, Holtz, RL, Skaritka, J, Fast, T, Sadananda, K, Lakshmipathye, M, and Tsakalakos, T (2005). "Strain profiling of fatigue crack overload effects using energy dispersive X-ray diffraction," *International Journal of Fatigue,* Vol 27, pp 1408–1419

Deslaef, D, Rouhaud, E, and Rasouli-Yazdi, S (2000). "3D Finite Element Models of Shot Peening Processes," *Fifth European Conference on Residual Stresses,* Trans Tech Publications, Materials Science Forum, Vol 347-349, pp 241-246

James, M, Hattingh, D, Hughes, D, Wei, LW, Patterson, E, and Quinta Da Fonseca, J (2004). "Synchrotron diffraction investigation of the distribution and influence of residual stresses in fatigue," *Fat & Fract. Engng. Mater. & Structures,* Vol 27, No 7, pp 609-622.

Kandil, FA, Lord, JD, Fry AT, and Grant, PV (2001). "A Review of Residual Stress Measurement Methods--A Guide to Technique Selection," *NPL Report No. MATC (A) 04,* National Physical Laboratory, Teddington, Middlesex, UK, TW11 0LW

Kuntz, T, Wadley, H, and Black, D (1993). "Residual strain gradient determination in metal-matrix composites by synchrotron x-ray energy dispersive diffraction," *Metall Trans A* , Vol 24, No 5, pp 1117–1124.

Lang M, and Marci, G (1999). "The influence of single and multiple overloads on fatigue crack propagation, " *Fatigue & Fracture of Engineering Materials & Structures,* Vol 22, No 4, pp. 257-271

Leggatt, R, Smith, D, Smith, S, and Faure, F (1996). "Development and experimental validation of the deep hole method for residual stress measurement," *J. Strain Anal, Eng. Des.*, Vol 31, No 3, pp 177-186

Makabe, C, Purnowidodo, A, and McEvily, AJ, (2004). "Effects of surface deformation and crack closure on fatigue crack propagation after overloading and underloading," *Int. J. Fatigue,* Vol 26, pp 1341-1438

Noroozi, AH, Glinka, G, and Lambert, S (2005). "A two parameter driving force for fatigue crack growth analysis," *Int. J. Fatigue,* Vol 27, pp 1277–1296

Prime, M, (1999). "Residual Stress Measurement by Successive Extension of a Slot: The Crack Compliance Method," *Appl. Mech. Rev.*, Vol 52, No 2, pp. 75-96.

Pyzalla, A (2000). "Methods and Feasibility of Residual Stress Analysis by High-Energy Synchrotron Radiation in Transmission Geometry Using a White Beam," *Journal of Nondestructive Evaluation,* Vol 19,pp 21-31

Ramos, M, Pereira, M, Dawish, F, Motta, S, and Carneir, M (2003). "Effect of single and multiple overloading on the residual fatigue life of a structural steel," *Fatigue & Fracture of Engineering Materials & Structures,* Vol 26, No 2, pp 115-125

Sadananda, K, Vasudevan, AK, Holtz, RL, and Lee, EU (1999). "Analysis of overload effects and related phenomena," *International Journal of Fatigue,* Vol 21, pp S233-S246.

Skorupa, M (1998). "Load interaction effects during fatigue crack growth under variable amplitude loading—a literature review. Part I: Empirical Trents," *Fat. Fract. Eng. Mat. Struct.*, Vol 21, No 8, pp. 987-1006

Skorupa, M (1999). "Load interaction effects during fatigue crack growth under variable amplitude loading—a literature review. Part II: qualitative interpretation," *Fat. Fract. Eng. Mat. Struct.*, Vol 22, No 10, pp 905-926

Steuwer, A, Santistebban, J, Withers, and Buslap, T (2004). "High-resolution strain mapping in bulk samples using full-profile analysis of energy dispersive synchrotron X-ray diffraction data," *J. Appl. Cryst.,* Vol 37, No 6, pp 883-889

Stoychev, S, and Kujawski, D (2005). "Analysis of crack propagation using ΔK and Kmax, " *International Journal of Fatigue* Vol 27, pp 1425–1431

Suresh, S (1998). *Fatigue of Materials*, Cambridge University Press, NY, pp. 305-306.

Tsakalakos, T, Croft, M, Zakharchenko, I, Zhong, Z, Gulak, Y, and Holtz, RL (2002). "On the Stability of Nanostructured Coatings by Synchrotron Radiation," AIAA-2002-1314, *43rd AIAA/ASME/ASCE/AHS/ASC Structures, Structural Dynamics, and Materials Conference,* Denver, Colorado, pp 1-10

Vasudevan, AK, Sadananda, K, and Louat, N (1994). "A review of crack closure, fatigue-crack threshold and related phenomena," *Mat. Sci. Eng. A,* Vol 188, No 1-2, pp 1-22

Verma B, and Ray, PK, (2002). "Fatigue crack growth retardation in spot heated mild steel sheet," *Bull. Mater. Sci.,* Vol 25, No 4, pp. 301–307.

Wang, H, Buchholz, F-G, Richard, HA, Jaag, S, and Scholtes, B (1999). "Numerical and experimental analysis of residual stresses for fatigue crack growth, " *Computational Materials Science*," Vol 16, No 1-4, pp 104-112

Withers, P, and Bhadeshia, H (2001). "Residual stress. Part 1 – Measurement techniques, " *Materials Science and Technology,* Vol 17, No 4, pp. 355-365